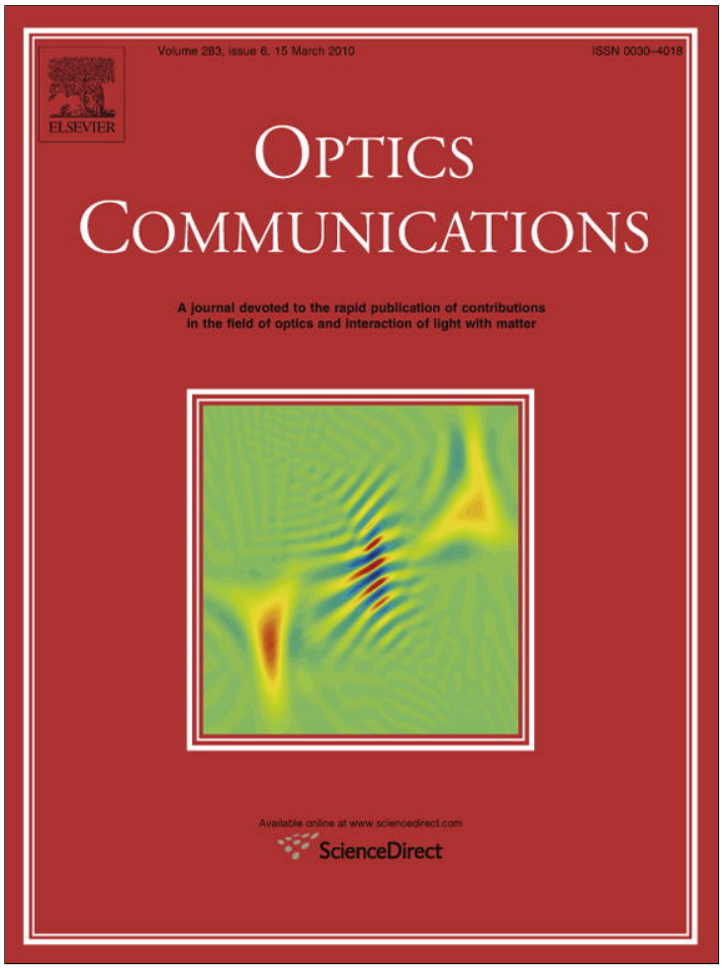

Optics Communications 283 (2010) 1200–1208

Contents lists available at ScienceDirect

Optics Communications

journal homepage: www.elsevier.com/locate/optcom

Influence of the order of the constituent basis matrices on the Mueller matrix decomposition-derived polarization parameters in complex turbid media such as biological tissues

Nirmalya Ghosh [a,*], Michael F.G. Wood [b,c], I. Alex Vitkin [b,c]

[a] IISER Kolkata, Mohanpur Campus, PO: BCKV Campus Main Office, Mohanpur 741252, West Bengal, India
[b] Ontario Cancer Institute, Division of Biophysics and Bioimaging, University Health Network, Canada M5G 2M9
[c] Department of Medical Biophysics and Radiation Oncology, University of Toronto, 610 University Avenue, Toronto, Ontario, Canada M5G 2M9

ARTICLE INFO

Article history:
Received 4 May 2009
Received in revised form 19 October 2009
Accepted 29 October 2009

ABSTRACT

The influence of the multiplication order of the constituent basis matrices on the Mueller matrix decomposition-derived polarization parameters in complex tissue-like turbid media exhibiting simultaneous scattering and polarization effects are investigated. A polarization sensitive Monte Carlo (MC) simulation model was used to generate Mueller matrices from turbid media exhibiting simultaneous linear birefringence, optical activity and multiple scattering effects. Mueller matrix decomposition was performed with different selected multiplication orders of the constituent basis matrices, which were further analyzed to derive quantitative individual polarization medium properties. The results show that for turbid medium having weak diattenuation (differential attenuation of two orthogonal polarization states), the decomposition-derived polarization parameters are independent of the multiplication order. Importantly, the values for the extracted polarization parameters were found to be in excellent agreement with the controlled inputs, showing self-consistency in inverse decomposition analysis and successful decoupling of the individual polarization effects. These results were corroborated further by selected experimental results from phantoms having optical (scattering and polarization) properties similar to those used in the MC model. Results from tissue polarimetry confirm that the magnitude of diattenuation is generally lower compared to other polarization effects, so that the demonstrated self-consistency of the decomposition formalism with respect to the potential ambiguity of ordering of the constituent matrices should hold in biological applications.

1. Introduction

Studies of polarization properties of scattered light from turbid media like biological tissues have received considerable attention because of their potential applications in diagnostic photomedicine [1,2]. The polarization parameters of light scattered from tissue contain rich morphological and functional information of potential biomedical importance. Despite the wealth of interesting properties that can be probed with polarized light, in optically thick turbid media such as tissues, numerous complexities due to multiple scattering and simultaneous occurrences of many polarization effects present formidable challenges. These include accurate measurement difficulties and extraction/unique interpretation of the constituent polarization parameters.

The Mueller matrix (transfer function of an optical system in its interactions with polarized light) contains complete information about all the polarization properties of a medium [3,4]. However, when many optical polarization effects occur simultaneously (as is the case for tissue where the most common polarimetry events are depolarization, linear birefringence and optical activity [2]), the resulting matrix elements reflect several 'lumped' effects, thus hindering extraction and unique interpretation of the constituent polarization parameters. A method to account for the effects of multiple scattering, and to decouple the individual contributions of simultaneously occurring polarization effects, is thus needed. Each of these, if separately extracted, holds promise as a useful biological metric. For example, chirality-induced optical rotation can be linked to the glucose concentration in the medium [5–8]; changes in tissue mechanical anisotropy (resulting from disease progression or treatment response) can be probed by linear birefringence (or retardance) measurements [9,10]. The individual constituent polarization properties can be extracted from the 'lumped' system Mueller matrix by performing polar decomposition of Mueller matrix. This decomposition methodology was first developed by Lu and Chipman [11]. Briefly, this approach consists

* Corresponding author. Tel.: +91 33 64513294; fax: +91 33 25873020.
E-mail address: nghosh@uhnres.utoronto.ca (N. Ghosh).

0030-4018/$ - see front matter © 2009 Elsevier B.V. All rights reserved.
doi:10.1016/j.optcom.2009.10.111

of representing a Mueller matrix **M**, obtained from an unknown system, as the product of three constituent 'basis' matrices, namely, a diattenuator followed by a retarder and a depolarizer. The validity of this decomposition procedure was demonstrated in optically *clear* media by Lu and Chipman. We have recently extended their analysis to encompass complex tissue-like turbid media, exhibiting simultaneous polarization effects in presence of multiple scattering [12,13]. Once calculated, the constituent matrices are further analyzed to derive individual polarization medium properties, namely, linear retardance (δ, and its orientation angle θ), optical rotation (ψ), diattenuation (d) and depolarization coefficient (Δ) [11,12]. Initial biomedical applications of this approach have also yielded very promising results [14,15].

However, an interesting problem that requires special care is that the multiplication order of the constituent basis matrices (depolarization, retardance and diattenuation) is ambiguous (due to the non-commuting nature of matrix multiplication), so that six different decompositions (order of multiplication) are possible [16]. It has been shown that the six different decompositions can be grouped in two families, depending upon the location of the depolarizer and the diattenuator matrices. Among the six decompositions, algorithms for two specific multiplication orders (one from each family) have been developed [17]. The other possible decompositions can be obtained using similarity transformations, for each of the two individual families [17]. The validity of these decompositions has been demonstrated in optical media where the polarization events are exhibited one after the other, as *sequential* multiplication implies [11,18]. However, in a complex random medium like biological tissue, no unique order can be assigned to these effects (optical activity due to chiral molecules, linear birefringence due to anisotropic tissue structures, and depolarization due to multiple scattering); rather, these are exhibited simultaneously. Thus it is necessary to investigate the influence of the multiplication order of the basis matrices on Mueller matrix decomposition from such complex system. More importantly, it is essential to know how the decomposition-derived polarization parameters are influenced by the selected multiplication order and whether the values of the derived parameters represent the *true* medium properties. We have therefore investigated these issues by decomposing Mueller matrices (whose constituent properties are controlled and are thus known *a priori*) generated with a polarization sensitive Monte Carlo simulation model (capable of simulating simultaneous scattering and polarization effects) [19] and also experimental Mueller matrices. The results of these investigations are reported in this paper.

The organization of this paper is as follows. The *forward* polarization sensitive Monte Carlo (MC) model and the *inverse* process for polar decomposition of the resulting Mueller matrices are described in Section 2. Section 3 briefly describes our experimental turbid-polarimetry system. The decomposition results of the MC-generated Mueller matrices from complex tissue-like turbid media (both in the forward and the backward detection geometry) and selected experimental results from biological tissues, are presented in Section 4. The paper concludes with a discussion on the biomedical utility of this promising Mueller matrix decomposition approach for quantitative tissue assessment.

2. Theory

2.1. Forward modeling of simultaneous occurrence of several polarization effects in turbid media using the Monte Carlo approach

Polarization sensitive Monte Carlo simulation model, developed and validated in our group [19,20], was used to generate the Mueller matrices of scattered light exiting the medium in both the forward and the backward direction. Similar to conventional intensity-based Monte Carlo models for light propagation in a multiply scattering medium [21,22], the photons are propagated between scattering events, as determined by pseudo random sampling of scattering mean free path. The photon propagates in the sample between scattering events a distance l sampled from the probability distribution $\exp(-\mu_t l)$. Here, the extinction coefficient μ_t is the sum of the absorption μ_a and scattering μ_s coefficients and l is the distance traveled by the photon between scattering events [22]. When the photon encounters a scattering event, a scattering plane and angle are statistically sampled based on the polarization state of the photon and the Mueller matrix of the scatterer. The photon's reference frame is first expressed in the scattering plane and then transformed to the laboratory (experimentally observable) frame through multiplication by a Mueller matrix calculated through Mie scattering theory [23]. The polarization information (in the form of Stokes vectors) is tracked for each photon packet. The scattering histories of a large number of such packets are tracked as they propagate through the medium and are summed to yield the macroscopic polarization parameters of interest (Stokes vectors, Mueller matrices, pathlength distributions, polarization statistics from different scattering histories, etc.).

Our Monte Carlo model has been extended to simulate the simultaneous effects of linear birefringence and optical activity in the presence of multiple scattering [19]. Note that this is not an obvious modeling step. Since matrix multiplication of the Mueller matrices are not commutative, different orders in which these effects are applied to the photon between scattering events will have different effects on the polarization. This was therefore accomplished by combining the effects into a single matrix describing them simultaneously, through the use of Jones *N*-matrix formalism [19,24]. Here, the matrix of the sample is represented as an exponential sum of differential matrices, known as *N*-matrices. Each matrix in this sum corresponds to a single optical property (e.g., linear birefringence or optical activity). These *N*-matrices are then used to express the matrix for the combined effect. Since matrix addition (unlike multiplication) is order independent, the ordering ambiguity is no longer an issue. The resulting matrix is applied to the photon between scattering events to model the simultaneous occurrence of linear birefringence and optical activity in a scattering medium. The model's testing and experimental validations have been reported previously [19].

Simulations were run for a set of input optical parameters of the scattering medium (μ_s and μ_a) exhibiting simultaneous linear and circular birefringence effects. Mie theory was used to compute the single scattering matrix for known diameter (D) and refractive index of scatterer (n_s) and refractive index of the surrounding medium (n_m). The wavelength of light (λ) was chosen to be $\lambda = 632.8$ nm. In the simulations, circular and linear birefringence were modeled through the optical activity χ in degrees per centimetre, and through the anisotropy in refractive indices (Δn), respectively. Here, $\Delta n (= n_e - n_o)$ is the difference in refractive index along the extraordinary axis (n_e) and the ordinary axis (n_o). For simplicity, it was assumed that the medium is uni-axial and that the direction of the extraordinary axis and the value for Δn is constant throughout the scattering medium. In each simulation, (e_s) and (n_o) were taken as input parameters and a specific direction of the extraordinary axis was chosen. As photons propagate between scattering events, the difference in refractive indices experienced by them depends on their propagation direction with respect to the extraordinary axis. The effect was modeled using standard formulae describing the angular variation of refractive index in uni-axial medium.

The Mueller matrices were generated for a 1-cm-thick slab of scattering medium having varying optical properties ($\mu_s, \Delta n$ and χ), for light exiting the medium through the forward or the back-

ward direction. The absorption was selected to be small (μ_a = 0.001 cm^{-1}) for all simulations. The photon collection geometry was chosen to have a detection area of 1 mm^2 and an acceptance angle of 20° (these parameters mimic our experimental turbid-polarimetry system [7,11,19]).

2.2. Polar decomposition of Mueller matrix

Having described the Monte Carlo approach to accurately *forward* model simultaneous polarization effects in the presence of multiple scattering, we now turn to the complicated *inverse* problem of separating out the constituent contributions from simultaneous polarization effects. That is, given a particular Mueller matrix obtained from an unknown complex system, can it be analyzed to extract constituent polarization contributions? Here, we shall discuss an extended Mueller matrix decomposition methodology that enables the extraction of the individual intrinsic polarimetry characteristics from the 'lumped' system Mueller matrix [11,12].

Polar decomposition method consists of decomposing a given Mueller matrix **M** into the product of three 'basis' matrices [11,12],

$$\mathbf{M} \Leftarrow \mathbf{M}_{\Delta} \cdot \mathbf{M}_{R} \cdot \mathbf{M}_{D} \tag{1}$$

with $\Leftarrow$ symbol used throughout the manuscript to signify the decomposition process. Here, a depolarizer matrix $\mathbf{M}_{\Delta}$ accounts for the depolarizing effects of the medium, a retarder matrix $\mathbf{M}_R$ describes the effects of linear birefringence and optical activity, and a diattenuator matrix $\mathbf{M}_D$ includes the effects of linear and circular diattenuation. The validity of such a decomposition was first demonstrated by Lu and Chipman in optically *clear* media [11]. We have recently extended and validated this approach for the analysis of complex random media [12,13].

As mentioned previously in the context of forward MC modeling, an important problem is that the multiplication order in Eq. (1) is ambiguous (due to the non-commuting nature of matrix multiplication, $\mathbf{M}_A\mathbf{M}_B \neq \mathbf{M}_B\mathbf{M}_A$), so that six different decompositions (orders of multiplication) are possible. The six different decompositions can be grouped in two families, depending upon the location of the depolarizer and the diattenuator matrices [11,16]. The three decompositions with the depolarizer set after the diattenuator form the first family (of which Eq. (1) is a particular sequence). On the other hand, the three decompositions with the depolarizer set before the diattenuator constitute the other family

$$\begin{array}{cc} (\mathbf{M}_{\Delta D}\ \text{family}) & (\mathbf{M}_{D\Delta}\ \text{family}) \\ \mathbf{M} \Leftarrow \begin{cases} \mathbf{M}_{\Delta}\mathbf{M}_{R}\mathbf{M}_{D} & (2.1) \\ \mathbf{M}_{\Delta}\mathbf{M}_{D}\mathbf{M}_{R} & (2.2) \\ \mathbf{M}_{R}\mathbf{M}_{\Delta}\mathbf{M}_{D} & (2.3) \end{cases} & \mathbf{M} \Leftarrow \begin{cases} \mathbf{M}_{D}\mathbf{M}_{R}\mathbf{M}_{\Delta} & (2.4) \\ \mathbf{M}_{R}\mathbf{M}_{D}\mathbf{M}_{\Delta} & (2.5) \\ \mathbf{M}_{D}\mathbf{M}_{\Delta}\mathbf{M}_{R} & (2.6) \end{cases} \end{array} \tag{2}$$

Among the six decompositions, algorithms for obtaining the basis matrices in Eq. (2.1) or for its reverse order (Eq. (2.4)), have been developed [17]. The other decompositions can be obtained using similarity transformations, for each of the two individual families [17]. We therefore remove these from further considerations and concentrate on decompositions using the orders of Eqs. (2.1) and (2.4).

Although the process for decomposition using the order of Eqs. (2.1) and (2.4) are qualitatively similar, there do exist important differences in the construction of the basis matrices and the derived polarization parameters. Specifically, the forms of the diattenuation ($\mathbf{M}_D$) and the depolarization ($\mathbf{M}_{\Delta}$) matrices are different. For the decomposition using the order of Eq. (2.1), $\mathbf{M}_D$ is constructed directly from the diattenuation vector $\vec{D}$ of the medium Mueller matrix **M** (1st row vector of **M**) as [11]

$$\mathbf{M}_D^{(1)} = \begin{bmatrix} 1 & \vec{D}^T \\ \vec{D} & m_D \end{bmatrix} \tag{3}$$

where the 3 × 3 sub-matrix m_D has the form defined in Ref. [11]. $\vec{D}$ is defined as

$$\vec{D} = \frac{1}{M(1,1)}[M(1,2)M(1,3)M(1,4)]^T \tag{4}$$

In contrast, for the decomposition using the order of Eq. (2.4), $\mathbf{M}_D$ is constructed from the polarizance vector $\vec{P}$ of the medium Mueller matrix **M** (1st column vector of **M**) as [17]

$$\mathbf{M}_D^{(4)} = \begin{bmatrix} 1 & \vec{P}^T \\ \vec{P} & m_P \end{bmatrix} \tag{5}$$

Here, $\vec{P}$ is defined as

$$\vec{P} = \frac{1}{M(1,1)}[M(2,1)M(3,1)M(4,1)]^T \tag{6}$$

These differences in $\mathbf{M}_D$ thus lead to a difference in the magnitude of diattenuation, derived via decomposition using the order of Eq. (2.1) or Eq. (2.4). In the former case, magnitude of diattenuation is extracted from the elements of first row of the medium Mueller matrix **M**; in the latter, it is calculated from the elements of first column.

Similarly, the forms of the depolarization matrices for decomposition using the orders of Eqs. (2.1) and (2.4) are [11,12,17]

$$\mathbf{M}_{\Delta}^{(1)} = \begin{bmatrix} 1 & \vec{0}^T \\ P_{\Delta} & m_{\Delta} \end{bmatrix} \tag{7}$$

and

$$\mathbf{M}_{\Delta}^{(4)} = \begin{bmatrix} 1 & \vec{D}_{\Delta}^T \\ \vec{0} & m_{\Delta} \end{bmatrix} \tag{8}$$

where the m_{Δ} is the 3 × 3 depolarization sub-matrix [11,13,17]. P_{Δ} and D_{Δ} are defined as

$$P_{\Delta} = \frac{\vec{P} - m\vec{D}}{1 - D^2}; \quad D_{\Delta} = \frac{\vec{D} - m\vec{P}}{1 - P^2} \tag{9}$$

Once decomposed (using the order of either Eq. (2.1) or Eq. (2.4)), these constituent matrices are further analyzed to derive individual polarization medium properties. Specifically, diattenuation (d, differential attenuation of orthogonal polarizations for linear and for circular polarization states), depolarization coefficients (Δ, linear and circular), linear retardance (δ, difference in phase between two orthogonal linear polarizations), and circular retardance or optical rotation (ψ, difference in phase between right and left circularly polarized light), can be determined from the decomposed basis matrices.

The magnitude of diattenuation (d) can be determined as [11,12]

$$d = \frac{1}{M_D(1,1)}\sqrt{M_D(1,2)^2 + M_D(1,3)^2 + M_D(1,4)^2} \tag{10}$$

Here, the coefficients $\mathbf{M}_D(1,2)$ and $\mathbf{M}_D(1,3)$ represent linear diattenuation for horizontal (vertical) and +45° (−45°) linear polarization respectively, and the coefficient $\mathbf{M}_D(1,4)$ represents circular diattenuation.

Next, depolarization is quantified through the depolarization matrix $\mathbf{M}_{\Delta}$ as the net depolarization coefficient Δ and linear

retardance δ and optical rotation ψ are calculated from the various elements of the retarder matrix $\mathbf{M}_R$ [12]. Specifically,

$$\Delta = 1 - \frac{|tr(\mathbf{M}_\Delta) - 1|}{3} \tag{11}$$

$$\delta = \cos^{-1}\left(\sqrt{(\mathbf{M}_R(2,2) + \mathbf{M}_R(3,3))^2 + (\mathbf{M}_R(3,2) - \mathbf{M}_R(2,3))^2} - 1\right) \tag{12}$$

$$\psi = \tan^{-1}\left(\frac{\mathbf{M}_R(3,2) - \mathbf{M}_R(2,3)}{\mathbf{M}_R(2,2) + \mathbf{M}_R(3,3)}\right) \tag{13}$$

In the present study, we have used both Eqs. (2.1) and (2.4) to decompose **M** and have investigated the influence of their respective multiplication order of the resulting constituent basis matrices on the derived polarization parameters (d, Δ, δ and ψ) from turbid media exhibiting simultaneous polarization effects.

3. Experimental method

The experimental Mueller matrices were recorded from dermal tissue of an athymic nude mouse (NCRNU-M, Taconic). The Mueller matrix was recorded *in vivo* from a dorsal skinfold window chamber mouse model, using a high sensitivity turbid-polarimetry system. The details of the measurement polarimeter and the window chamber model are provided in Refs. [7,12,19,15] respectively.

Briefly, our turbid-polarimetry system employs polarization modulation using a photoelastic modulator (Hinds Instruments IS-90) and synchronous lock-in detection (Stanford Research Systems, SR830), allowing sensitive low-noise measurements of the Stokes vector of the light interacting with a turbid sample [7] in various geometries. By cycling the polarization of the incident beam (HeNe laser, 15 mW, $\lambda = 632.8$ nm) using a linear polarizer and quarter wave-plate combination, and measuring the output Stokes vectors, the Mueller matrix of the sample can be constructed [12].

In the window chamber model, the skin layer of the mouse was removed from a 10 mm diameter region on the dorsal surface, and a titanium saddle was sutured in place to hold the skin flap vertically [15]. A protective glass coverslip (145 ± 15 μm thick) was placed over the exposed tissue plane. This allowed for direct *in vivo* optical transmission measurements of polarized light through the ~500 μm thick tissue layer. Mueller matrices were recorded from the tissue in the forward detection (transmission) geometry (detection area of 1 mm^2 and an acceptance angle ~20° around the direction of the ballistic beam).

4. Results and discussion

4.1. Sequential occurrence of polarization effects

We begin our investigation on simpler system, where the polarization events (depolarization, retardance and diattenuation) are exhibited one after the other as *sequential* multiplication implies. We shall construct Mueller matrix of such media for known intrinsic polarization properties and decompose them with multiplication order of the constituent basis matrices opposite (reverse order decomposition) to that used for constructing the original Mueller matrix. The idea is to identify the sources of error in such reverse order decomposition process, and to understand the influence of the individual medium polarization properties on the resulting error (clearly, decomposition in the *same* order as was used to construct the original matrix yields a trivial self-consistent result). We multiply depolarization, retardance (combined effect of both linear and circular retardance) and diattenuation matrices, to generate the system **M** what will be subject to decomposition analysis. The chosen constituent matrices are

$$\mathbf{M}_\Delta = \begin{bmatrix} 1 & 0 & 0 & 0 \\ 0 & 0.8 & 0 & 0 \\ 0 & 0 & 0.7 & 0 \\ 0 & 0 & 0 & 0.6 \end{bmatrix};$$

$$\mathbf{M}_R = \begin{bmatrix} 1 & 0 & 0 & 0 \\ 0 & 0.8148 & 0.1619 & -0.5567 \\ 0 & 0.3187 & 0.6770 & 0.6634 \\ 0 & 0.4843 & -0.7180 & 0.5000 \end{bmatrix}; \tag{14}$$

$$\mathbf{M}_D^1 = \begin{bmatrix} 1 & 0.1 & 0 & 0 \\ 0.1 & 1 & 0 & 0 \\ 0 & 0 & 0.99 & 0 \\ 0 & 0 & 0 & 0.99 \end{bmatrix}; \quad \mathbf{M}_D^2 = \begin{bmatrix} 1 & 0.8 & 0 & 0 \\ 0.8 & 1 & 0 & 0 \\ 0 & 0 & 0.6 & 0 \\ 0 & 0 & 0 & 0.6 \end{bmatrix}$$

Here, the retardance matrix was constructed [3,11] with input linear retardance value of $\delta = 1.04$ rad (orientation angle of retarder axis $\theta = 20°$ and optical rotation value of $\psi = 3°$. Two different diattenuation matrices were used [3], one with low magnitude of diattenuation ($\mathbf{M}_D^1$, magnitude of diattenuation $d = 0.1$) and the other with high magnitude of diattenuation ($\mathbf{M}_D^2$, magnitude of diattenuation $d = 0.8$). In both cases, the axis of diattenuation was along the horizontal direction. We shall consider two cases, (i) Mueller matrix constructed with weak diattenuation ($\mathbf{M} = \mathbf{M}_\Delta\mathbf{M}_R\mathbf{M}_D^1$), (ii) Mueller matrix constructed with strong diattenuation ($\mathbf{M} = \mathbf{M}_\Delta\mathbf{M}_R\mathbf{M}_D^2$).

Table 1 shows the medium Mueller matrix for combination of a weak diattenuator ($d = 0.1$), followed by a retarder and a depolarizer ($\mathbf{M} = \mathbf{M}_\Delta\mathbf{M}_R\mathbf{M}_D^1$) and the corresponding decomposed basis matrices, using the reverse order ($\mathbf{M} \Leftarrow \mathbf{M}_D\mathbf{M}_R\mathbf{M}_\Delta$) decomposition process. Eqs. (10)–(13) were applied to the decomposed basis matrices to retrieve the individual polarization parameters (d, Δ, δ and ψ). The determined values for these are also listed in Table 1. The determined values for the parameters Δ, δ and ψ, shows excellent agreement with the controlled inputs (the derived basis matrices are also in excellent agreement with the corresponding input constituent matrices). Marginal error is observed in the value for diattenuation d.

Note that the reverse order decomposition results in small but non-zero values for the off-diagonal elements of the decomposition-derived depolarization matrix $\mathbf{M}_\Delta$ (thus differing from the input depolarization matrix used to construct the medium Mueller matrix). We have observed that diagonalized representation of the inner 3×3 depolarization sub-matrix (m_Δ of Eqs. (7) and (8)) corrects for these elemental errors in the derived depolarization matrix $\mathbf{M}_\Delta'$. In Table 1, we have therefore shown both forms of the depolarization matrices. Henceforth, for all the decomposition results presented in this paper, we shall present the diagonalized form representation of the depolarization matrix. Results of decomposition on Mueller matrices having other varying intrinsic medium polarization parameters confirmed that for medium having weak diattenuation effects (magnitude of diattenuation $d \leqslant 0.1$), the decomposition-derived polarization parameters are not significantly influenced by the choice of the multiplication order of the basis matrices in the decomposition process.

The basic reason why for low enough diattenuation, the decomposition-derived polarization parameters are ~ independent of the multiplication order can be understood from the following arguments. In absence of diattenuation (i.e., if $\mathbf{M} = \mathbf{M}_\Delta\mathbf{M}_R$), if one uses the similarity transformation $\mathbf{M}_\Delta = \mathbf{M}_R\mathbf{M}_\Delta^{\mathbf{r}}(\mathbf{M}_\mathbf{R}^{-1})$, the input matrix becomes $\mathbf{M}_R\mathbf{M}_\Delta^{\mathbf{r}}$. This form of the input Mueller matrix is then the same as that of the reverse order ($\mathbf{M} \Leftarrow \mathbf{M}_\Delta\mathbf{M}_R$) used in the decomposition process. Indeed, the results of reverse order decomposition ($\mathbf{M} \Leftarrow \mathbf{M}_\Delta\mathbf{M}_R$) of Mueller matrix constructed with no

Table 1
Top: The generated Mueller matrix (**M**) for combination of a weak diattenuator (magnitude of diattenuation $d = 0.1$), followed by a retarder and a depolarizer ($\mathbf{M} = \mathbf{M}_{\Delta}\mathbf{M}_R\mathbf{M}_D^1$) and the decomposed basis matrices. The Mueller matrix was decomposed using the reverse order ($\mathbf{M} \Leftarrow \mathbf{M}_D\mathbf{M}_R\mathbf{M}_{\Delta}$) decomposition process. The decomposition-derived depolarization matrix in diagonalized form (M'_{Δ}) is shown separately in the 3rd row. Bottom: The input control values for the polarization parameters (2nd column). The values for the polarization parameters extracted from the decomposed matrices (3rd column).

$$\mathbf{M} = \begin{pmatrix} 1.0000 & 0.1000 & 0 & 0 \\ 0.0652 & 0.6518 & 0.1289 & -0.4431 \\ 0.0223 & 0.2231 & 0.4715 & 0.4621 \\ 0.0291 & 0.2906 & -0.4286 & 0.2985 \end{pmatrix}$$

$$\mathbf{M_{\Delta}} = \begin{pmatrix} 1.0000 & 0.0443 & -0.0065 & 0.0100 \\ 0 & 0.7396 & 0.0479 & -0.0695 \\ 0 & 0.0479 & 0.6497 & 0.0268 \\ 0 & -0.0695 & 0.0268 & 0.7045 \end{pmatrix} \quad \mathbf{M_R} = \begin{pmatrix} 0 & 0 & 0 & 0 \\ 0 & 0.8146 & 0.1621 & -0.5570 \\ 0 & 0.3188 & 0.6771 & 0.6633 \\ 0 & 0.4846 & -0.7178 & 0.4998 \end{pmatrix} \quad \mathbf{M_D} = \begin{pmatrix} 1.0000 & 0.0652 & 0.0223 & 0.0291 \\ 0.0652 & 0.9993 & 0.0007 & 0.0009 \\ 0.0223 & 0.0007 & 0.9974 & 0.0003 \\ 0.0291 & 0.0009 & 0.0003 & 0.9976 \end{pmatrix}$$

$$\mathbf{M'_{\Delta}} = \begin{pmatrix} 1.0000 & 0.0443 & -0.0065 & 0.0100 \\ 0 & 0.7973 & 0 & 0 \\ 0 & 0 & 0.5982 & 0 \\ 0 & 0 & 0 & 0.6983 \end{pmatrix}$$

Parameters	Input values	Estimated values
d	0.1	0.075
Δ	0.30	0.302
ψ	3°	2.997°
δ, θ	1.04 rad, 20°	1.047 rad, 20.01°

Table 2
Top: The generated Mueller matrix (**M**) for combination of a strong diattenuator ($d = 0.2$), followed by a retarder and a depolarizer ($\mathbf{M} = \mathbf{M}_{\Delta}\mathbf{M}_R\mathbf{M}_D^2$) and the decomposed basis matrices. The Mueller matrix was decomposed using the reverse order ($\mathbf{M} \Leftarrow \mathbf{M}_D\mathbf{M}_R\mathbf{M}_{\Delta}$) decomposition process. Bottom: The input control values for the polarization parameters (2nd column).The values for the polarization parameters extracted from the decomposed matrices (3rd column).

$$\mathbf{M} = \begin{pmatrix} 1 & 0.8000 & 0 & 0 \\ 0.5215 & 0.6518 & 0.0777 & -0.2672 \\ 0.1785 & 0.2231 & 0.2843 & 0.2786 \\ 0.2325 & 0.2906 & -0.2585 & 0.1800 \end{pmatrix}$$

$$\mathbf{M_{\Delta}} = \begin{pmatrix} 1 & 0.5493 & -0.0486 & 0.0744 \\ 0 & 0.3761 & 0 & 0 \\ 0 & 0 & 0.5054 & 0 \\ 0 & 0 & 0 & 0.5555 \end{pmatrix} \quad \mathbf{M_R} = \begin{pmatrix} 1 & 0 & 0 & 0 \\ 0 & 0.7868 & 0.1847 & -0.5889 \\ 0 & 0.3257 & 0.6863 & 0.6503 \\ 0 & 0.5242 & -0.7035 & 0.4798 \end{pmatrix} \quad \mathbf{M_D} = \begin{pmatrix} 1 & 0.5215 & 0.1785 & 0.2325 \\ 0.5215 & 0.9523 & 0.0517 & 0.0673 \\ 0.1785 & 0.0517 & 0.8190 & 0.0230 \\ 0.2325 & 0.0673 & 0.0230 & 0.8314 \end{pmatrix}$$

Parameters	Expected values	Estimated values
d	0.80	0.60
Δ	0.30	0.52
ψ	3.0°	2.73°
$\delta\theta$	1.04 rad, 20°	1.07 rad. 19.6°

diattenuation ($\mathbf{M} = \mathbf{M}_{\Delta}\mathbf{M}_R$) yielded complete agreement between the extracted polarization parameters and the controlled inputs, as expected.

Table 2 displays the medium Mueller matrix for combination of a strong diattenuator ($d = 0.8$), followed by a retarder and a depolarizer ($\mathbf{M} = \mathbf{M}_{\Delta}\mathbf{M}_R\mathbf{M}_D$) and the corresponding decomposed basis matrices. The Mueller matrix was again decomposed using the reverse order [Eq. (2.4), $\mathbf{M} \Leftarrow \mathbf{M}_D\mathbf{M}_R\mathbf{M}_{\Delta}$] decomposition process.

Comparison of the derived and the input control values for the polarization parameters reveals, that unlike case (i), for this medium with strong diattenuation, reverse order decomposition yields significant errors in all the retrieved polarization parameters. The largest errors were observed in the value for diattenuation d and net depolarization coefficient Δ (column 3). The source of these errors can be identified by noting that in case of decomposition using the order of Eq. (2.4) ($\mathbf{M} \Leftarrow \mathbf{M}_D\mathbf{M_R}\mathbf{M}_{\Delta}$), the diattenuation parameter d is extracted from the first column of the medium Mueller matrix **M**. For the medium Mueller matrix constructed using the opposite (to that used in decomposition process) order of multiplication of the constituent matrices (i.e., with Eq. (2.1), $\mathbf{M} = M_{\Delta}\mathbf{M}_R\mathbf{M}_D$), while the first row remains unaffected and is the same as that of the diattenuation matrix $\mathbf{M}_D$, the first column is significantly altered due to multiplication of the other two constituent matrices ($\mathbf{M}_{\Delta}$ and $\mathbf{M}_R$). This results in erroneous estimation of the diattenuation parameter and subsequently introduces errors in the elements of the derived diattenuation matrix $\mathbf{M}_D$. This error is carried forward to the derived basis matrices $\mathbf{M}_{\Delta}$ and $\mathbf{M_R}$, and thus in the corresponding polarization parameters (Δ, δ and ψ)

extracted from these matrices. Similar decomposition analyses [using the orders of either Eq. (2.1) or Eq. (2.4)] were also performed on medium Mueller matrices constructed using other selected multiplication orders of the constituent basis matrices. In all cases, diattenuation was identified as the major source of errors in the extracted polarization parameters. Results of decomposition on Mueller matrices having other varying intrinsic medium polarization parameters also yielded similar results and confirmed that for medium having strong diattenuation effects (magnitude of diattenuation $d \geqslant 0.2$), reverse order decomposition results in significant errors in all the retrieved polarization parameters.

4.2. Simultaneous occurrence of polarization effects

Having investigated the possible sources of errors in the decomposition-derived medium polarization properties of simpler (sequential) systems, we now turn to the more complex, tissue-like turbid media that exhibit simultaneous polarization effects in the presence of multiple scattering.

Table 3 shows the Monte Carlo simulation-generated Mueller matrix and the decomposed basis matrices for a birefringent (anisotropy in refractive index $\Delta n = 1.36 \times 10^{-5}$, that corresponds to a value of $\delta = 1.34$ radian for a path length of 1 cm), chiral (optical activity $\chi = 1.96^\circ\ \mathrm{cm}^{-1}$), turbid medium (scattering coefficient $\mu_s = 30\ \mathrm{cm}^{-1}$, thickness = 1 cm) comprised of monodispersed spherical scatterers ($D = 1.40\ \mu\mathrm{m}$, $n_s = 1.59$, $n_m = 1.34$, anisotropy parameter $g = 0.935$). These results are for light exiting the medium through the forward direction, along the ballistic beam direction. The axis of linear birefringence was kept along the vertical direction ($\theta = 90^\circ$) in the simulation. The constituent basis matrices obtained via decomposition with the order of Eq. (2.1) ($\mathbf{M} \Leftarrow \mathbf{M}_\Delta \mathbf{M}_R \mathbf{M}_D$) and Eq. (2.4) ($\mathbf{M} \Leftarrow \mathbf{M}_D \mathbf{M}_R \mathbf{M}_\Delta$) are shown in the 2nd and the 3rd rows respectively. The determined values for the polarization parameters are also listed in the table.

The expected values for linear retardance δ and optical rotation ψ were calculated from the input control values for birefringence (Δn) and optical activity (χ) and were corrected for increased pathlength due to multiple scattering (the MC-generated average photon pathlength of light exiting the medium in the forward direction was 1.30 cm) [25]. The expected value for net depolarization coefficient Δ was obtained from the results of MC simulation of an analogous purely depolarizing turbid medium ($\mu_s = 30\ \mathrm{cm}^{-1}$) with no birefringence ($\Delta n = 0$) or optical activity ($\chi = 0^\circ\ \mathrm{cm}^{-1}$).

Several interesting trends can be noted. Both the decompositions yield very small but non-zero value of d. In absence of any intrinsic diattenuation property of the medium, the only other source of diattenuation is the scattering-induced diattenuation that primarily arises from singly (or weakly) scattered photons [26]. Since multiply scattered photons are the dominant contributors to the detected signal in the forward detection geometry, the scattering-induced diattenuation effect is also expected to be very weak [12]; this probably accounts of the small but non-zero values of the diattenuation. Note that in its absence (or for weak diattenuation), decomposition using either of the two selected multiplication orders of the basis matrices yields almost identical results. This suggests that for media having weak diattenuation effects (including complex turbid media that exhibit simultaneous polarization effects in presence of multiple scattering), the decomposition-derived polarization parameters are $\sim$ independent of the multiplication order of the basis matrices.

The other three derived polarization parameters (Δ, ψ and δ) are also found to be in excellent agreement with the controlled inputs. The decomposition-derived value of Δ closely resembles that for an analogous purely depolarizing turbid medium. This implies that decomposition process successfully decouples the depolarization effects due to multiple scattering from linear retardation and optical rotation contributions, thus yielding accurate and quantifiable estimates of the δ and ψ parameters in the presence of turbidity. The derived value for δ (=1.41 rad) is, however, slightly lower than one would expect for average photon path length of 1.30 cm ($\delta = 1.74$ rad). In our previous paper [12], it was shown that this lowering of the value of δ arises because the scattered

Table 3
Top: The Monte Carlo simulation-generated Mueller matrix and the decomposed basis matrices for a birefringent (anisotropy in refractive index $\Delta n = 1.36 \times 10^{-5}$, that corresponds to a value of $\delta = 1.34$ radian for a path length of 1 cm), chiral (optical activity $\chi = 1.96^\circ\ \mathrm{cm}^{-1}$), turbid medium (scattering coefficient $\mu_s = 30\ \mathrm{cm}^{-1}$, anisotropy parameter $g = 0.935$, thickness = 1 cm), in the forward detection geometry. The constituent basis matrices obtained via decomposition with the order of Eq. (2.1) ($\mathbf{M} \Leftarrow \mathbf{M}_\Delta \mathbf{M}_\mathbf{D} \mathbf{M}_R$) and Eq. (2.4) ($\mathbf{M} \Leftarrow \mathbf{M}_D\, \mathbf{M}_R \mathbf{M}_\Delta$) are shown in the 2nd and the 3rd rows respectively. Bottom: The expected values for the polarization parameters (2nd column). The values for the polarization parameters extracted from the decomposed matrices (3rd and 4th column).

$$\mathbf{M} = \begin{pmatrix} 1 & 0.0025 & 0.0048 & 0.0023 \\ 0.0007 & 0.6346 & 0.0309 & -0.0304 \\ -0.0003 & -0.0319 & 0.0496 & -0.6966 \\ -0.0005 & -0.0296 & 0.7075 & 0.1730 \end{pmatrix}$$

$$\mathbf{M}_\Delta = \begin{pmatrix} 1 & 0 & 0 & 0 \\ -0.0010 & 0.6360 & 0 & 0 \\ 0.0011 & 0 & 0.6504 & 0 \\ -0.0042 & 0 & 0 & 0.7728 \end{pmatrix} \quad \mathbf{M}_R = \begin{pmatrix} 1 & 0 & 0 & 0 \\ 0 & 0.9977 & 0.0505 & -0.0447 \\ 0 & -0.0520 & 0.1552 & -0.9865 \\ 0 & -0.0429 & 0.9866 & 0.1574 \end{pmatrix} \quad \mathbf{M}_D = \begin{pmatrix} 1 & 0.0025 & 0.0048 & 0.0023 \\ 0.0025 & 1 & 0 & 0 \\ 0.0048 & 0 & 1 & 0 \\ 0.0023 & 0 & 0 & 1 \end{pmatrix}$$

$$\begin{pmatrix} 1 & 0.0020 & 0.0051 & 0.0022 \\ 0 & 0.6360 & 0 & 0 \\ 0 & 0 & 0.6503 & 0 \\ 0 & 0 & 0 & 0.7728 \end{pmatrix} \quad \begin{pmatrix} 1 & 0 & 0 & 0 \\ 0 & 0.9977 & 0.0505 & -0.0447 \\ 0 & -0.0520 & 0.1552 & -0.9865 \\ 0 & -0.0429 & 0.9866 & 0.1574 \end{pmatrix} \quad \begin{pmatrix} 1 & 0.0007 & -0.0003 & -0.0005 \\ 0.0007 & 1 & 0 & 0 \\ -0.0003 & 0 & 1 & 0 \\ -0.0005 & 0 & 0 & 1 \end{pmatrix}$$

Parameters	Expected values	Estimated values using the order of Eq. (2.1)	Estimated values using the order of Eq. (2.4)
d	0	0.006	0.001
Δ	0.30	0.313	0.313
ψ (°)	2.57	2.54	2.54
δ (rad)	1.74	1.41	1.41

light does not travel in a straight line but rather along many possible zig-zag paths. Since a component of such curved propagation paths is along the direction of the linear birefringence axis, this leads to a reduction in net linear retardance δ (because propagation along the direction of the birefringence axis does not yield any retardance).

Experimental studies on phantoms (developed using polyacrylamide as a base medium, with polystyrene microspheres to create turbidity, sucrose to induce optical activity, and mechanical stretching to cause linear birefringence [19]) having controlled sample polarizing properties but without diattenuation (thus analogous to properties used in the MC model) also yielded similar self-consistency in decomposition analysis (results not shown here). In agreement with the MC results, the extracted polarization parameters were found to be $\sim$ independent of the selected multiplication order of the basis matrices (difference in their values was in the range 1–5%) and were in excellent agreement with the controlled inputs [12].

The decomposition results presented above were for Mueller matrices recorded from turbid medium in the forward detection geometry, where the scattering-induced diattenuation effects are weak [12,26]. However, in the backward detection geometry (a geometry that may be advantageous for *in situ* measurements), *for off-axis detection*, the scattering-induced artifacts are more coupled with the intrinsic polarization parameters, partly because of the increasing contribution of the singly or weakly backscattered photons. Differences in amplitude and phase between the singly (or weakly) backscattered light polarized parallel and perpendicular to the scattering plane manifest as scattering-induced diattenuation and linear retardance [8,13,26]. Indeed, decomposition of Mueller matrices recorded from birefringent, chiral turbid medium at detection positions sufficiently close to the exact backscattering direction [*off-axis detection*, radial distance $r < l_{tr}$, l_{tr} is the transport scattering length = $1/\mu_s(1-g)$], resulted in erroneous estimation of the intrinsic values for δ and ψ of the medium, due to the interference of the scattering-induced artifacts (results not shown here) [13]. Importantly, due to presence of strong scattering-induced diattenuation ($d \geqslant 0.2$), significant differences were observed in the polarization parameters extracted via decompositions using the two different selected multiplication orders [orders of Eqs. (2.1) and (2.4)] of the basis matrices, none yielding satisfactory agreement with the control inputs. Our studies have shown that as one moves away from the exact backscattering direction, the magnitude of scattering-induced diattenuation and retardance gradually diminish and become weak ($d \leqslant 0.05$, $\delta \leqslant 0.1$) for detection positions located at distances larger than $\sim$ a transport length away from the point of illumination ($r > l_{tr}$) [13].

In Table 4, we show the MC-generated Mueller matrix and the decomposed basis matrices for a birefringent ($\Delta n = 1.36 \times 10^{-5}$), chiral ($\chi = 1.96^\circ\ \mathrm{cm}^{-1}$), turbid medium ($\mu_s = 60\ \mathrm{cm}^{-1}$, $g = 0.935$, thickness = 1 cm). The results are shown for scattered light collected at a spatial position 5 mm ($r > l_{tr}, l_{tr} = 2.56$ mm) away from the point of illumination in the backscattering geometry.

As expected, the scattering-induced diattenuation effect is observed to be weak, although the magnitude ($d \sim 0.02$) is slightly higher than that observed in the forward detection geometry. Importantly, as for the forward detection geometry, decomposition using either of the two selected multiplication orders of the basis matrices [Eqs. (2.1) and (2.4)] yields essentially identical values for the retrieved polarization parameters. The derived value of Δ (=0.798) was once again found to be close to that ($\Delta = 0.763$) for an analogous purely depolarizing turbid medium (same turbidity, no birefringence nor chirality), implying successful decoupling of depolarization effects. The values for both δ and ψ, in the backscattering geometry, are, however, significantly lower than one would expect for the MC-generated average photon path length of 1.53 cm.

This does not originate due to any error in the decomposition analysis. As noted in our previous study [13], contribution of the (singly or weakly) backscattered photons accounts for the lower value of ψ in the backward detection geometry. For the backscattered photons (that suffer scattering in the backward hemisphere only), the net rotation value partly cancels out due to a change in the handedness of rotation, thus reducing the value for net optical rotation ψ

Table 4
Top: The Monte Carlo simulation-generated Mueller matrix and the decomposed basis matrices for a birefringent (anisotropy in refractive index $\Delta n = 1.36 \times 10^{-5}$, that corresponds to a value of $\delta = 1.34$ rad for a path length of 1 cm), chiral (optical activity $\chi = 1.96^\circ\ \mathrm{cm}^{-1}$), turbid medium (scattering coefficient $\mu_s = 60\ \mathrm{cm}^{-1}$, anisotropy parameter $g = 0.935$, thickness = 1 cm), in the backward detection geometry. The results are shown for scattered light collected at a spatial position 5 mm ($r > l_{tr}$) away from the point of illumination in the backscattering geometry. The constituent basis matrices obtained via decomposition with the order of Eq. (2.1) ($\mathbf{M} \Leftarrow \mathbf{M}_\Delta \mathbf{M}_R \mathbf{M}_D$) and Eq. (2.4) ($\mathbf{M} \Leftarrow \mathbf{M}_D \mathbf{M}_R \mathbf{M}_\Delta$) are shown in the 2nd and the 3rd rows respectively. Bottom: The values for the polarization parameters extracted from the decomposed matrices.

$$\mathbf{M} = \begin{pmatrix} 1 & -0.0167 & -0.0019 & -0.0095 \\ -0.0190 & 0.1273 & 0.0075 & -0.0058 \\ 0.0009 & -0.0054 & 0.0302 & -0.1853 \\ 0.0024 & -0.0051 & 0.1901 & 0.2648 \end{pmatrix}$$

$$\mathbf{M}_\Delta = \begin{pmatrix} 1 & 0 & 0 & 0 \\ -0.0169 & 0.1215 & 0 & 0 \\ -0.0009 & 0 & 0.1275 & 0 \\ 0.0052 & 0 & 0 & 0.3562 \end{pmatrix} \quad \mathbf{M}_R = \begin{pmatrix} 1 & 0 & 0 & 0 \\ 0 & 0.9978 & 0.0591 & -0.0290 \\ 0 & -0.0593 & 0.6159 & -0.7856 \\ 0 & -0.0286 & 0.7856 & 0.6181 \end{pmatrix} \quad \mathbf{M}_D = \begin{pmatrix} 1 & -0.0167 & -0.0019 & -0.0095 \\ -0.0167 & 1 & 0 & 0 \\ -0.0019 & 0 & 0.9998 & 0 \\ \mathbf{-0.0095} & \mathbf{0} & \mathbf{0} & \mathbf{0.9999} \end{pmatrix}$$

$$\begin{pmatrix} 1 & -0.0143 & -0.0022 & -0.0101 \\ 0 & 0.1215 & 0 & 0 \\ 0 & 0 & 0.1275 & 0 \\ 0 & 0 & 0 & 0.3561 \end{pmatrix} \quad \begin{pmatrix} 1 & 0 & 0 & 0 \\ 0 & 0.9978 & 0.0591 & -0.0289 \\ 0 & -0.0593 & 0.6159 & -0.7856 \\ 0 & -0.0286 & 0.7856 & 0.6181 \end{pmatrix} \quad \begin{pmatrix} 1 & -0.0190 & 0.0009 & 0.0024 \\ -0.0190 & 1 & 0 & 0 \\ 0.0009 & 0 & 0.9998 & 0 \\ 0.0024 & 0 & 0 & 0.9998 \end{pmatrix}$$

Parameters	Estimated values using the order of Eq. (2.1)	Estimated values using the order of Eq. (2.4)
d	0.0193	0.0191
Δ	0.0798	0.798
ψ (°)	2.1	2.1
δ (rad)	0.90	0.90

[13]. As was the case of the forward detection geometry, components of the curved propagation paths that are along the direction of linear birefringence axis lead to a reduction in the net linear retardance δ. Since, on an average, the curvature of the propagation paths is greater for photons exiting the medium through the backward direction as compared to those exiting through the forward direction, this linear retardance reduction effect is more pronounced in the backscattering geometry.

The results of simulations for other varying scattering and polarization parameters [varied in the range; linear retardance δ: 0–2 rad, optical rotation ψ: 0–5°, scattering coefficient μ_s: 0–100 cm $^{-1}$, (resulting in net depolarization Δ: 0–0.9), these values roughly encompass the ranges typically found in biological tissue] were also similar to the results presented above. Thus, for complex turbid media exhibiting simultaneous polarization events (but having weak diattenuation, $d(\leqslant 0.1)$, the decomposition-derived polarization parameters are $\sim$ independent of the selected multiplication order of the basis matrices in the decomposition process, and also represent true medium properties. Note that although many biological molecules (such as amino acids, proteins, nucleic acids) exhibit dichroism or diattenuation, the overall magnitude is much lower compared to the other effects. The extracted polarization parameters are therefore expected to be independent of the selected multiplication order of the basis matrices in actual tissues. In order to confirm this, we present selected experimental polarimetry results from *in vivo* tissue and test the performance of the polar decomposition method.

Table 5 shows the experimental Mueller matrix and the corresponding decomposed basis matrices from dermal tissue of an athymic nude mouse. The Mueller matrix was recorded in transmission *in vivo* from a dorsal skinfold window chamber mouse model. The determined values for the polarization parameters [for decompositions using the orders of Eqs. (2.1) and (2.4)] are also listed in Table 5.

Careful examination of the experimental Mueller matrix **M** reveals several important features. The diattenuation effects are observed to be slightly stronger than for the previously examined simulated turbid media. This is possibly due to contribution of some intrinsic diattenuation (dichroism) of tissue, in addition to the weak scattering-induced diattenuation. However, the overall diattenuation effect is quite weak (elemental values of the first row or the first column of the medium Mueller matrix < 0.1). Further, the differences between the values for the matrix elements of first row and first column of **M** are also not that significant. This suggests that even if there is some diattenuation effect present in the medium, it does not exhibit in a preferred sequence. This follows because multiplication of the diattenuation matrix in any preferred order should result in a difference in the elemental values of first row and first column of the resulting Mueller matrix (as was the case for the sequential effects matrix shown in Table 2). Decomposition using either of the two-selected multiplication orders of the basis matrices therefore yields almost identical values for the retrieved polarization parameters (marginal difference is observed in the value for d only; the other parameters Δ, ψ and δ are almost identical).

As expected, the derived decomposition value for d is found to be very low. Conversely, the value for δ is quite high $\sim$1.06 rad). Presence of anisotropic structures like collagen fibers can attribute to the observed significant birefringence (retardance) levels in the skin tissue. In fact, using the approximate light pathlength, $l \approx 500$ μm (the true pathlength will be somewhat longer due to scattering [25]), the intrinsic birefringence $\Delta n (= \delta\lambda/2\pi l)$ was estimated to be $\approx 2.0 \times 10^{-4}$. This birefringence level is reasonably close to those found in the literature for tissue birefringence, typically $\sim 1 \times 10^{-3}$ [27]. The extracted value of net depolarization coefficient is $\Delta \sim 0.58$. From the MC-generated depolarization values (simulation of the experiment), the scattering coefficient μ_s of the tissue was approximated to be $\sim$170 cm^{-1}, which is also in reasonable agreement with literature values [22]. Similar to phantom studies, the extracted polarization parameters of the *in vivo* tissue therefore appear to represent *true* medium properties.

Results of polarimetry studies on various other types of tissues (rat myocardium, brain, liver tissues) also yielded similar self-consistent results. As was the case for turbid phantoms exhibiting weak diattenuation effects (*MC-simulated* or *experimentally* measured), in tissues with diattenuation ($d \leqslant 0.1$), the decomposition-derived

Table 5
Top: The experimental Mueller matrix and the decomposed basis matrices from dermal tissue of an athymic nude mouse. The Mueller matrix was recorded *in vivo* from a dorsal skinfold window chamber mouse model [15], using a high sensitivity turbid-polarimetry system [7]. The constituent basis matrices obtained via decomposition with the order of Eq. (2.1) ($\mathbf{M} \Leftarrow \mathbf{M}_\Delta \mathbf{M}_R \mathbf{M}_D$) and Eq. (2.4) ($\mathbf{M} \Leftarrow \mathbf{M}_D M_R M_\Delta$) are shown in the 2nd and the 3rd rows respectively. Bottom: The values for the polarization parameters extracted from the decomposed matrices.

M

1	0.0707	0.0348	-0.0060
0.0480	0.4099	0.0077	0.0650
0.0162	-0.0184	0.2243	-0.3580
0.0021	-0.0465	0.3571	0.1783

$\mathbf{M}_\Delta$

1	0	0	0
0.0193	0.4006	0	0
0.0076	0	0.4596	0
-0.0060	0	0	0.3768

$\mathbf{M}_R$

1	0	0	0
0	0.9935	0.0697	0.0897
0	0.0435	0.4960	-0.8673
0	-0.1049	0.8655	0.4897

$\mathbf{M}_D$

1	0.0707	0.0348	-0.0060
0.0707	0.9994	0.0012	0
0.0348	0.0012	0.9975	0
-0.0060	0	0	0.9969

1	0.0516	0.0301	-0.0037
0	0.3994	0	0
0	0	0.4588	0
0	0	0	0.3758

1	0	0	0
0	0.9935	0.0701	0.0898
0	0.0436	0.4960	-0.8672
0	-0.1047	0.8655	0.4898

1	0.0480	0.0162	0.0021
0.0480	0.9999	0.0004	0
0.0162	0.0004	0.9988	0
0.0021	0	0	0.9987

Parameters	Estimated values using the order of Eq. (2.1)	Estimated values using the order of Eq. (2.4)
d	0.079	0.051
Δ	0.58	0.59
ψ (°)	0.51	0.50
δ (rad)	1.06	1.058

polarization parameters were essentially $\sim$ independent of the selected multiplication order of the basis matrices in the decomposition process, showing self-consistency in decomposition analysis.

5. Conclusions

In summary, we have investigated the influence of the multiplication order of the constituent basis matrices on the Mueller matrix decomposition-derived polarization parameters in complex tissue and tissue-like turbid media exhibiting simultaneous scattering and polarization effects. The results demonstrate that for turbid media having weak diattenuation, the extracted polarization parameters are $\sim$ independent of the selected multiplication order of the basis matrices in the decomposition process, and also represent *true* medium properties. Similarly, Mueller matrix measurements and analysis of biological tissue showed that since the diattenuation effects are also weak, the decomposition formalism is self-consistent with respect to the potential ambiguity of ordering. This approach thus appears to be valid in tissue. Individual tissue polarimetry effects can therefore be successfully decoupled and quantified despite their simultaneous occurrence, even in the presence of the numerous complexities due to multiple scattering. The ability to isolate individual polarization properties provides a potentially valuable non-invasive tool for tissue characterization. We are currently exploring application of this approach in two scenarios of significant clinical interest, that for monitoring regenerative treatments of the heart and for non-invasive glucose measurements, with early indications showing promise and warranting further studies [14]. We are also expanding our investigations of *in vivo* biomedical deployments of this promising method [15].

References

[1] V.V. Tuchin, L. Wang, D. Zimnyakov, Optical Polarization in Biomedical Applications, Springer-Verlag, Berlin, Heidelberg, NY, 2006.
[2] L.V. Wang, G.L. Coté, S.L. Jacques, J. Biomed. Opt. 7 (2002) 278.
[3] R.A. Chipman, Polarimetry, in: M. Bass (Ed.), Handbook of Optics, second ed., vol. 2, McGraw-Hill, New York, 1994, pp. 22.1–22.37. Chap. 22.
[4] C. Brosseau, Fundamentals of Polarized Light: A Statistical Optics Approach, Wiley, New York, 1998.
[5] V.V. Tuchin (Ed.), Handbook of Optical Sensing of Glucose in Biological Fluids and Tissues, CRC Press, Taylor & Francis Group, London, 2009.
[6] R.J. Mc Nichols, G.L. Cote, J. Biomed. Opt. 5 (2000) 5.
[7] X. Guo, M.F.G. Wood, I.A. Vitkin, J. Biomed. Opt. 11 (2006) 041105.
[8] D. Côté, I.A. Vitkin, Opt. Express 13 (2005) 148.
[9] P.J. Wu, J.T. Walsh Jr., J. Biomed. Opt. 11 (2006) 014031.
[10] J.F. de Boer, T.E. Milner, J. Biomed. Opt. 7 (2002) 359.
[11] S. Yau Lu, R.A. Chipman, J. Opt. Soc. Am. A 13 (1996) 1106.
[12] N. Ghosh, M.F.G. Wood, I.A. Vitkin, J. Biomed. Opt. 13 (2008) 044036.
[13] N. Ghosh, M.F.G. Wood, I.A. Vitkin, J. Appl. Phys. 105 (10) (2009) 102023.
[14] N. Ghosh, M.F.G. Wood, S.H. Li, R.D. Weisel, B.C. Wilson, Ren-Ke Li, I.A. Vitkin, J. Biophotonics 2 (3) (2009) 145.
[15] M.F.G. Wood, N. Ghosh, E.H. Moriyama, B.C. Wilson, I.A. Vitkin, J. Biomed. Opt. 14 (2009) 014029.
[16] J. Morio, F. Goudail, Opt. Lett. 29 (2004) 2234.
[17] R. Ossikovski, A. De Martino, S. Guyot, Opt. Lett. 32 (2007) 689.
[18] M. Anastasiadou, S.B. Hatit, R. Ossikovski, S. Guyot, A. De Martino, J. Eur. Opt. Soc.: Rapid Publications 2 (2007) 07018.
[19] M.F.G. Wood, X. Guo, I.A. Vitkin, J. Biomed. Opt. 12 (2007) 014029.
[20] D. Côté, I.A. Vitkin, Pol-MC: A Three Dimensional Polarization Sensitive Monte Carlo Implementation for Light Propagation in Tissue, available online at <http://www.novajo.ca/ont-canc-instbiophotonics/>.
[21] L. Wang, S.L. Jacques, L. Zheng, Comput. Methods Programs Biomed. 47 (1995) 131.
[22] A.J. Welch, M.J.C. van Gemert, Optical–Thermal Response of Laser Irradiated Tissue, Plenum Press, New York, 1995.
[23] C.F. Bohren, D.R. Huffman, Absorption and Scattering of Light by Small Particles, Wiley, New York, 1983. Chap. 2.
[24] R. Clark Jones, J. Opt. Soc. Am. 38 (1948) 671.
[25] X. Guo, M.F.G. Wood, I.A. Vitkin, Opt. Express 15 (2007) 1348.
[26] S. Manhas, M.K. Swami, P. Buddhiwant, N. Ghosh, P.K. Gupta, K. Singh, Optics Express 14 (2006) 190.
[27] W. Wang, L.V. Wang, Propagation of polarized light in birefringent media: a Monte Carlo study, J. Biomed. Opt. 7 (2002) 350.